frontiers in Marine Science

TYPE Original Research
PUBLISHED 21 July 2026
DOI 10.3389/fmars.2026.1846069

OPEN ACCESS

EDITED BY
Borja Aguiar-González,
University of Las Palmas de Gran Canaria, Spain

REVIEWED BY
Tien Anh Tran,
Seoul National University, Republic of Korea
Malek Belgacem,
National Research Council (CNR), Italy
Simone Sammartino,
University of Malaga, Spain
Evi Bourma,
Hellenic Centre for Marine Research, Greece

*CORRESPONDENCE
Pierre-Marie Poulain
ppoulain@ogs.it

RECEIVED 02 April 2026
REVISED 29 June 2026
ACCEPTED 29 June 2026
PUBLISHED 21 July 2026

CITATION
Poulain P-M, Notarstefano G, Gallo A and Mauri E (2026) Assessing Mediterranean Sea temperature and salinity trends using Argo float data and reanalysis products between 2012 and 2025. *Front. Mar. Sci.* 13:1846069. doi: 10.3389/fmars.2026.1846069

Assessing Mediterranean Sea temperature and salinity trends using Argo float data and reanalysis products between 2012 and 2025

Pierre-Marie Poulain*, Giulio Notarstefano, Antonella Gallo and Elena Mauri

National Institute of Oceanography and Applied Geophysics, Trieste, Italy

This study compares temperature and salinity changes in the Mediterranean Sea over the period 2012–2025, using Argo float profiles and operational reanalysis products in three open-sea regions: the Western Mediterranean, Ionian, and Levantine basins. The temporal evolution of conservative temperature and absolute salinity is examined using Hovmöller diagrams (time–depth), and linear regression is applied to quantify long-term trends. The results reveal consistent and significant warming in the Western Mediterranean and Ionian Sea, with trends reaching 0.8-0.9 °C per decade near the surface. In contrast, a negative salinity trend (up to -0.2 g kg^{-1} per decade) in the upper 100 m is observed, likely linked to the freshening of the North Atlantic. The intermediate layers associated with Levantine Intermediate Water exhibit a clear increase in salinity, up to 0.1 g kg^{-1} per decade, indicating ongoing modification of this key Mediterranean water mass. While significant discrepancies arise in the upper water column of the Ionian and Levantine seas due to sparser and intermittent Argo coverage and higher variability, both datasets consistently indicate warming and salinification below 800 m. Near the surface, reanalysis temperature trends significantly exceed those found with Argo data in both the Ionian and Levantine seas. In contrast, Argo salinity trends are larger compared to reanalysis in the upper Levantine Sea, but they are comparable in the surface Ionian. Overall, these findings confirm that the Mediterranean Sea continues to experience significant warming and subsurface salinification, and that these trends can be effectively monitored by Argo floats, provided sufficient spatial coverage across all subbasins. The persistence of these trends through 2025 highlights the continuing impact of global climate change on the Mediterranean thermohaline structure.

KEYWORDS
Mediterranean Sea, profiling floats, reanalysis, salinity, temperature, trend

1 Introduction

Over recent decades, the Mediterranean region has emerged as a prominent climate "hotspot," exhibiting a particularly strong response to global climate change (Giorgi, 2006). The Mediterranean Sea plays a crucial role in modulating this regional response since a warming climate induces not only an increase in sea temperature but also a rise in salinity driven by enhanced evaporation.

Mediterranean sea warming and salinification trends were explored initially using ship-based *in situ* measurements. For instance, the deep waters of the Western Mediterranean were shown to become warmer and saltier since the 1950s (Béthoux et al., 1990; Krahmann and Schott, 1998; Millot, 2007). Borghini et al. (2014) found that the temperature and salinity of the deep waters of the Western Mediterranean Sea increased by about 0.4 °C and 0.15 psu per decade, respectively, between 1961 and 2008. These trends were attributed to deep-water formation events and the downward flux of heat and salt facilitated by salt-finger mixing. Vargas-Yáñez et al. (2017) also found similar positive trends in the intermediate and deep Spanish waters for the period 1943-2015. More recently, Margirier et al. (2020) using data mostly provided by gliders reported trends of 0.6 °C and 0.12 psu per decade for the Levantine Intermediate Water (LIW) at intermediate depths in the northwestern Mediterranean basin for the period 2007-2017, and confirmed the deep vertical transport of heat and salt content by deep convection events.

The salinity variability and water cycle of the Mediterranean Sea were investigated by Skliris et al. (2018) using historical observations and reanalysis products since 1950. Their results indicated a basin-scale salinification, particularly pronounced in the intermediate and deep layers, primarily driven by changes in the regional water cycle.

Trends in Mediterranean Sea Surface Temperature (SST) were also quantified using satellite observations. The Mediterranean SST was shown to increase since the early 1980s, with warming rates of approximately 0.4 °C per decade (Nykjaer, 2009; Skliris et al., 2012; Mohamed et al., 2019; Pastor et al., 2020; Pisano et al., 2020; Juza and Tintoré, 2021; García-Monteiro et al., 2022), substantially exceeding the global ocean average (Merchant et al., 2025). This warming is not spatially uniform: SST trends generally increase from the western to the eastern Mediterranean, with rates below 0.3 °C per decade in the western basin and above 0.4 °C per decade in the eastern basin (Skliris et al., 2012; Pisano et al., 2020; Pastor et al., 2020). Recently, the years 2024 and 2025 were recorded as the hottest in over four decades, with basin-wide heat storage reaching unprecedented levels due to a combination of global warming and acute, multi-month marine heatwaves (Napolitano et al., 2025).

More recently, the temperature and salinity trends were studied more globally in the Mediterranean Sea using Argo float data (Kassis and Korres, 2020; Fedele et al., 2022; Kubin et al., 2023; Chevillard et al., 2024) or operational products (Aydogdu et al., 2023; Escudier et al., 2025). Argo data between 2004 and 2017 were utilized by Kassis and Korres (2020) to study the thermohaline properties in the central and eastern Mediterranean basins. Positive long-term trends were generally confirmed for both temperature and salinity, and deviations were interpreted in terms of the variability in the circulation and the main water masses. Fedele et al. (2022) focused on the near-surface Atlantic Water (AW) and intermediate LIW and estimated trends in the entire Mediterranean and its main subbasins for the period 2001-2019. AW temperature trends of 0.54, 0.23 and 0.26 °C per decade were found for the Algerian, Ionian and Levantine areas, respectively. For the LIW, the temperature trend ranged between 0.1 and 0.3 °C per decade. In terms of salinity, the LIW trend was rather small (0.02-0.04 psu/decade) whereas the AW trend resulted negative in the Algerian and Catalan subbasins, reaching -0.13 psu per decade. Argo float data were also analyzed by Kubin et al. (2023), who reported a mean warming trend of approximately 0.4 °C per decade in the upper 700 m of the Mediterranean over the period 2005–2020. When the analysis was restricted to the Western basin, the estimated warming rate increased substantially, reaching about 0.7 °C per decade.

Aydogdu et al. (2023) used reanalysis products from the Copernicus Marine Service (CMS) to investigate salinity changes in the upper Mediterranean Sea. Their results indicated an increase in salinity over recent decades between the surface and 300 m depth, with stronger trends in the eastern basin (~0.1 psu per decade), thereby confirming the findings of Skliris et al. (2018). In the western basin, negative trends were identified in localized areas, attributed either to local upwelling processes or to the influence of freshening North Atlantic waters (Holliday et al., 2020).

Finally, Chevillard et al. (2024) used Mediterranean Argo data in 2013–2022 and reported warming trends being highest in the western Mediterranean from surface to depth, and salinification trends being highest in the upper layer of the Levantine subbasin. They also used the CMS reanalysis products to show that the Mediterranean Argo is adequate to capture the thermohaline variability in most subbasins at seasonal and interannual scales.

The most recent analysis of the CMS reanalysis products (Escudier et al., 2025) demonstrated a general warming and salinification of the Mediterranean Sea, with rates reaching up to 0.5 °C per decade and 0.2 psu per decade, respectively, since the turn of the century. Positive temperature and salinity anomalies were shown to propagate downward within the water column to depths of approximately 1000 m.

The primary objective of this study is to assess the observational adequacy of the Argo network for accurately capturing basin-scale long-term trends in temperature and salinity through comparison with CMS reanalysis products. A second objective is to quantify thermal and haline trends in selected open-sea regions of the Mediterranean Sea using non-uniformly sampled Argo float data over the period 2012–2025, and to characterize their vertical structure down to approximately 2000 m depth.

Although the study shares thematic similarities with Chevillard et al. (2024), it adopts a distinct analytical approach and a different temporal framework, focusing directly on temperature and salinity profiles. Moreover, this paper extends the works of Fedele et al. (2022) and Kubin et al. (2023) using the Argo dataset updated until 2025. Details of the Mediterranean Argo float data, the CMS products, and the data processing methodology are provided in Section 2. Long-term trends are presented and compared in Section 3, and the results are discussed in relation to previous studies in Section 4.

2 Data and methods

The observational dataset for this study is derived from the Argo profiling float network (Argo float data and metadata from Global Data Assembly Centre (Argo GDAC), 2026; Wong et al., 2020) within the Mediterranean Sea, covering the period from 1 January 2012 to 30 September 2025 and extending in the water column from the surface (typically near 3 dbar) to a maximum of 2000 dbar. Argo data in the Mediterranean Sea are available prior to this period (Poulain et al., 2007) and extend to greater depths; however, they are too sparse to allow the computation of robust statistics. The year 2012 marks the beginning of several national Argo programs in the Mediterranean under the framework of the Euro-Argo European Research Infrastructure, and corresponds to a significant increase in the number of floats deployed in this marginal sea. The initial dataset comprised 83395 profiles collected by 453 floats, consisting of both Delayed Mode Quality Control (DMQC) data (mainly before 2022) and Real-Time (RT) data (mainly in 2022-2025). The standard accuracy of DMQC'ed data is 0.002 °C for temperature and 0.01 psu for salinity. While the temporal resolution between successive profiles for individual floats varied from 3 hours to 10 days, the majority of the sampling followed a standard cycle of approximately 5 days (Poulain et al., 2007). The vertical sampling resolution typically ranged between 1 dbar in the top layer and 50 dbar at depth.

To ensure the robustness of the trend analysis, the following processing approach was implemented. The initial dataset was first reduced to 75795 profiles (from 444 floats) by retaining only those containing both temperature and salinity data at least one depth. Pressure measurements were converted to depth using the hydrostatic equation, and the vertical profiles were binned from 10 to 2000 m using a 10-m interval. *In situ* temperature and practical salinity were converted to conservative temperature (Θ) and absolute salinity (S_A) according to the Thermodynamic Equation Of Seawater – 2010 (TEOS-10) standards. For comparison with historical results, Θ closely matches *in situ* temperature, while S_A differs from practical salinity by an approximately constant offset of about 0.2, with negligible impact on trend estimates. In order to subsample the floats with short cycles and render the dataset more uniformly sampled in time, linear interpolation in time was applied with exactly 5-day resolution for each individual float. Time series were truncated if a data gap exceeded 100 days. This interpolation partly filters out high-frequency variability possibly produced by internal waves, although the interpolated profiles can remain contaminated by these processes, especially in the western Alboran Sea near the Strait of Gibraltar where internal tides prevail. Following these rigorous quality control and interpolation steps, the final processed dataset utilized for trend estimation consists of 61755 profiles, about 81% of the initial number of profiles. Despite these processing steps, the dataset remains affected by spatial and temporal sampling heterogeneity, which may introduce biases in the estimation of mean properties and long-term trends. Indeed, spatial coverage across the Mediterranean basin is non-uniform, as evidenced by the distribution of profile counts in 0.5° × 0.5° bins (Figure 1), with the highest densities occurring in the northwestern Mediterranean, the Adriatic Sea, and the eastern Ionian Sea. In the latter region, the number of interpolated profiles exceeded 400 per bin, as floats became trapped within a strong anticyclonic gyre (the Pelops Eddy, see Robinson et al., 1991) for extended periods. The number of float profiles is minimum in the southern and southeastern areas, mainly because of the limited deployments in these areas.

The processed Argo float dataset was analyzed in three distinct open-sea regions: the Western Mediterranean Sea (WMED), the Ionian Sea (IONIAN), and the Levantine Sea (LEVANTINE). These regions are shown in Figure 1, and their boundaries are listed in Table 1. All regions have comparable areas (approximately 200000 km²) and are characterized by water depths mostly exceeding 1000 m. They were selected to minimize geographical variability and to exclude coastal influences, in particular to reduce river runoff effects. Among the three regions, WMED is the most densely sampled, with 8513 5-day interpolated profiles provided by 124 floats. The IONIAN region has 5467 processed profiles mostly concentrated in the northern part, while the LEVANTINE region includes 5565 interpolated profiles (Table 1). Argo sampling across the regions is clearly non-uniform in time. Figure 2 shows the

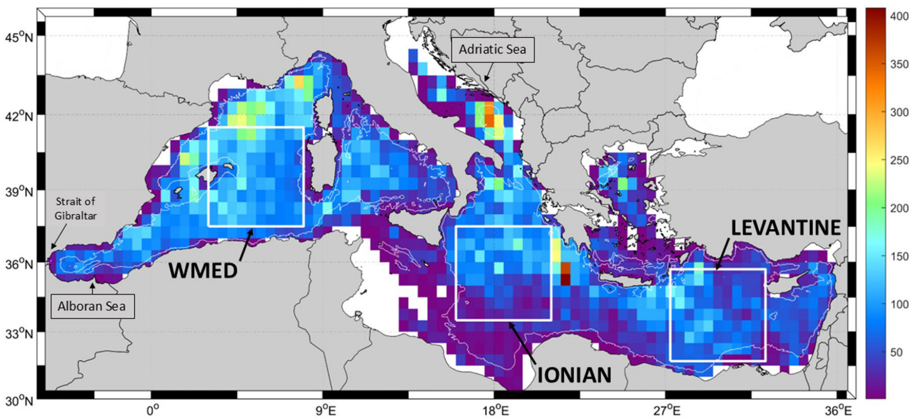

FIGURE 1
Density of 5-day interpolated Argo profiles in the Mediterranean Sea between 1 January 2012 and 30 September 2025 (number of profiles in 0.5° x 0.5° bins). The open-sea areas considered in this work are shown with white squares in the major western, central and eastern Mediterranean subbasins. The 1000-m isobaths are shown in white.

TABLE 1 **Numbers of Argo profiles and floats between 1 January 2012 and 30 September 2025 in the regions WMED, IONIAN and LEVANTINE regions of the Mediterranean Sea (see squares in Figure 1 and text for definitions).**

Region	Longitudes	Latitudes	Number of floats	Number of profiles	Number of 5-day profiles	Number of ind. profiles
WMED	3°-8°E	37°30'-41°30'N	124	9771	8513	7942
IONIAN	16°-21°E	33°30'-37°30'N	83	8064	5467	5004
LEVANTINE	27°15'-32°15'E	31°42'-35°42'N	67	7430	5565	4881

number of distinct floats and 5-day interpolated profiles in 10-day intervals as a function of time in the three regions. Sampling peaks in summer 2015, with 64 profiles from 32 floats. From 2023 onward, the number of floats and profiles becomes sparse in the LEVANTINE region, whereas sampling in WMED increases, reaching 37 profiles from 20 floats in August 2025.

The CMS Mediterranean Sea Physics Reanalysis (Escudier et al., 2020, 2021) is a product generated by a numerical system combining a hydrodynamic model, provided by the Nucleus for European Modelling of the Ocean (NEMO), with a variational data assimilation scheme (OceanVAR) for temperature and salinity vertical profiles. The assimilated observations include ship-based conductivity-temperature-depth sensors, expendable bathythermographs, satellite along-track Sea Level Anomaly data and Argo float data down to 2000 m depth (Oddo et al., 2026). The model has a horizontal resolution of 1/24° (~4–5 km) and 141 unevenly spaced vertical levels. Daily CMS temperature and salinity products were downloaded in December 2025 from the CMS website. For simplicity, only the data corresponding to the 5th, 15th, and 25th of each month between 1 September 2012 and 25 September 2025 were extracted, representing the three 10-day periods of each month. The similarity between the Argo profiles and the CMS data sampled at the Argo locations and times was assessed for the year 2015, which was selected because of the high availability of Argo observations (see Appendix 1).

Long-term trends were derived using the same procedure for both the Argo data and CMS reanalysis products.

Spatio-temporal variability was first examined qualitatively using Hovmöller contour diagrams of mean Θ and S_A as functions of depth and time, on a grid with 10-day and 10-m intervals for each region. Gaps in the data were filled by linear interpolation in two dimensions. Selected isotherms and isohaline curves were overlaid after additional smoothing using a moving average of 180 days in time and 50 m in depth.

Quantitative trend slopes were also determined using spatially averaged values within the WMED, IONIAN, and LEVANTINE regions and temporally averaged values in 10-day intervals. Trend slopes were determined at the CMS standard depths between 10 and 1945 m for both the Argo and CMS datasets. First, within each 10-day interval, Argo profiles separated by less than approximately 10 km were excluded in order to retain more independent observations. This simple procedure resulted in an approximately 10% reduction in the number of profiles within the regions (see Table 1). Similarly, CMS profiles were subsampled with a horizontal resolution of ~10 km (1/12°). Second, the seasonal cycle was estimated through linear regression and removed from the time series. Third, a standard linear least-squares fit was applied to determine the long-term trends. Confidence intervals for the slopes were computed assuming N−2 degrees of freedom, where N is the number of observations (Emery and Thomson, 2024). Despite the application of 10 km filtering and 10-day binning, some profiles may still exhibit correlation. Consequently, this can lead to an underestimation of the confidence intervals. The coefficient of determination (R^2) was calculated to assess the goodness of fit of the linear model. Weighted least-squares fitting (with weights proportional to the number of observations within each 10-day interval for each region), and standard least-squares fitting applied to individual (independent) profiles were also applied for comparison (see

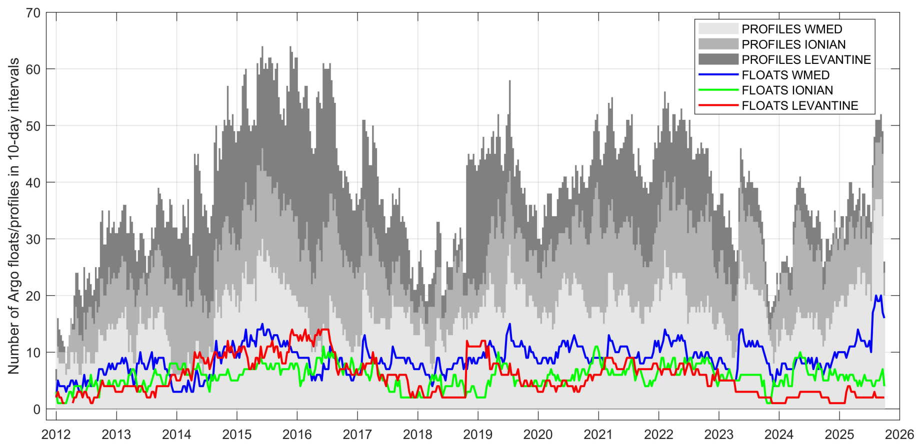

FIGURE 2
Number of 5-day interpolated Argo profiles (grey stacked bars), and corresponding number of individual floats (colored lines), in the Mediterranean Sea, in 10-day intervals between 1 January 2012 and 30 September 2025, for the WMED, IONIAN and LEVANTINE areas.

Appendix 2). Note that, after subsampling at 1/12° resolution, the CMS dataset contains approximately 3000 profiles within each geographical region every 10 days. This can be compared with the number of Argo profiles shown in Figure 2, which reaches at most about 30 profiles per region. As a result, the Argo sampling represents only about 1% of the CMS sampling and is also highly variable in time as well as spatially inhomogeneous within each region.

The sensitivity of the trend results with respect to the size of the selected regions was also explored by considering areas slightly extended or reduced (see Appendix 3).

3 Results

3.1 Hovmöller diagrams

The temporal evolution of Θ and S_A in the three open-sea regions is first examined between the surface and 2000 m depth, using Hovmöller diagrams derived from both Argo data and CMS products (Figures 3–8). Seasonal temperature variability within the surface mixed layer, extending to approximately 100 m depth, is evident in all regions. In the LEVANTINE region, seasonal salinity variations are also pronounced, with near-surface maxima occurring during the second half of the year, occasionally overlying a salinity minimum that extends down to about 150 m depth (Figure 8). Seasonal variability in the Mediterranean Sea is not discussed further here, as the focus of this study is on long-term trends.

Below the surface mixed layer, the WMED is stratified, with Θ gradually decreasing to 12.9–13.0 °C in the 1000–2000 m layer (Figure 3). The isotherms progressively deepen over time, reflecting warming of the water column. In terms of salinity, the WMED is characterized by a subsurface maximum near 300 m associated with the LIW, with S_A > 38.85 g kg^{-1} (Figure 4). Below this level, S_A decreases to about 38.7 g kg^{-1}. The salinity of the LIW core increases with time, and the underlying isohalines generally deepen. The spatio-temporal patterns and trends are qualitatively consistent between the Argo and CMS datasets.

Below 200 m, the IONIAN region is stratified, with Θ decreasing to 13.4–13.5 °C in the 1000–2000 m layer (Figure 5). Isotherms also tend to deepen slightly over time, although the trend is less clear than in the WMED. The LIW salinity maximum is located between 200 and 400 m, reaching values of S_A up to 39.25 g kg^{-1} (Figure 6). Beneath this layer, S_A decreases to approximately 38.85 g kg^{-1} between 1000 and 2000 m. As in the WMED, LIW salinity increases over time, and the deeper isohalines descend. Argo and CMS results are generally comparable.

The LEVANTINE region is strongly stratified between 200 and 800 m in both temperature and salinity (Figures 7, 8). Θ decreases with depth to about 13.5 °C, and isotherms show slight downward

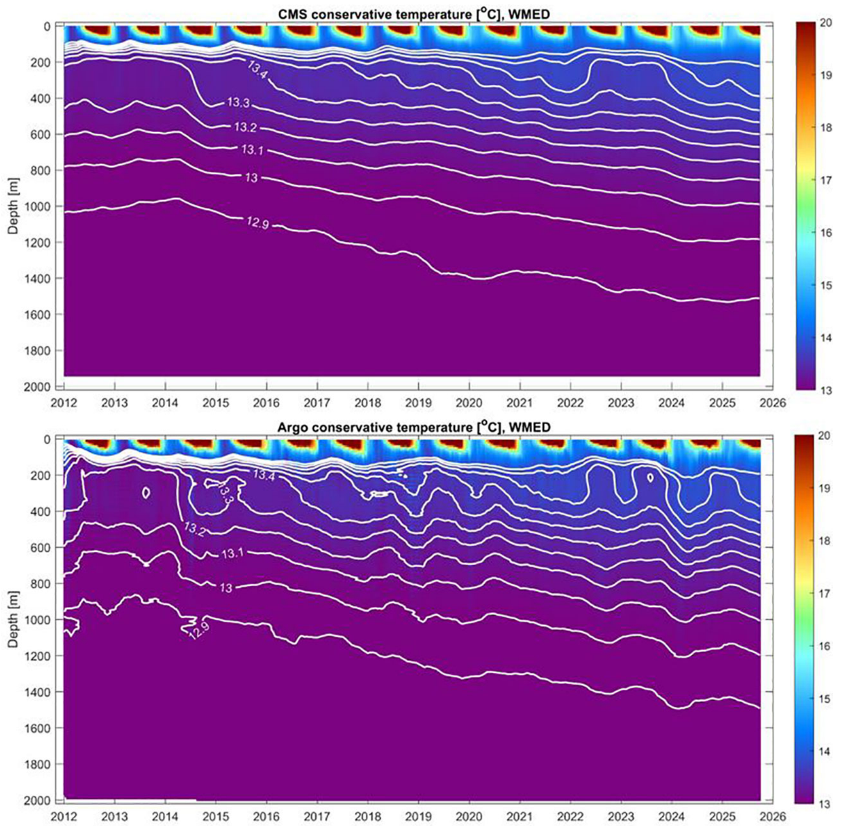

FIGURE 3
Hovmöller diagram of conservative temperature Θ versus time and depth in the open-sea western Mediterranean area (WMED), derived from the CMS reanalysis (top) and Argo data (bottom). Contour interval is 0.1°C between 12.9 and 13.9°C.

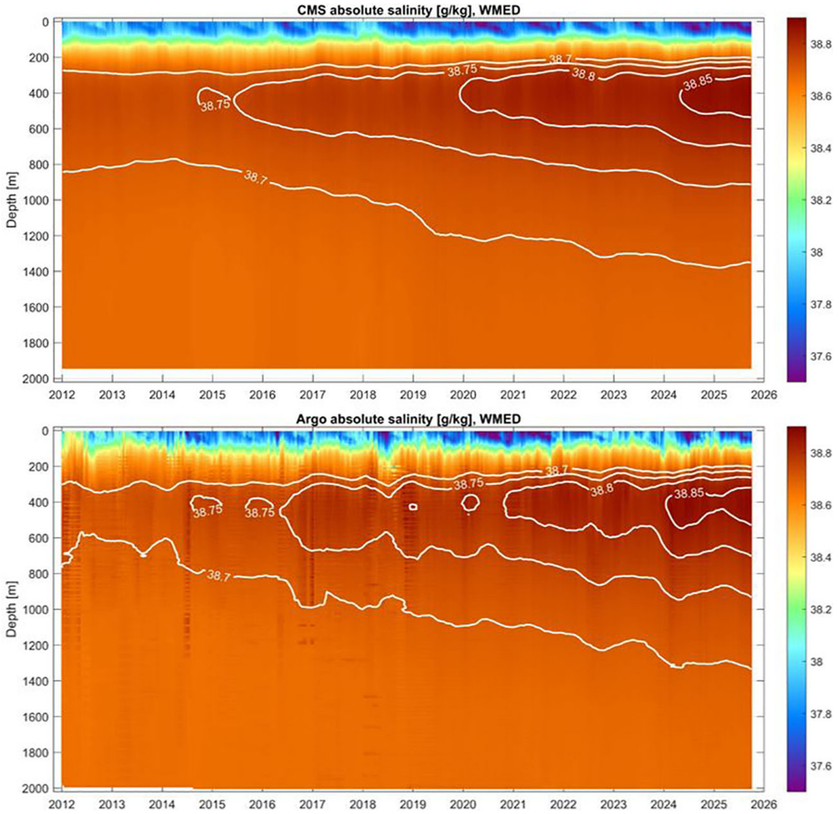

FIGURE 4
Same as Figure 3, but for absolute salinity S_A. Contour interval is 0.05 g kg^{-1} between 38.7 and 38.85 g kg^{-1}.

displacement over time (Figure 7). The LIW core is shallower, near 200 m, and S_A decreases to approximately 39.0 g kg^{-1} down to about 600 m depth (Figure 8). The LIW salinity exhibits two temporal maxima, between 2017 and 2022 and again in 2025. Argo results appear relatively noisy, and long-term salinity trends are not evident. In particular, salinity increases above 800 m depth in late 2024 and early 2025, associated with a single float trapped in the Mersa Matruh anticyclonic eddy (Robinson et al., 1991). In contrast, CMS indicates slight salinification between 500 and 800 m.

3.2 Long-term linear trends

Linear trends were fitted on the Argo and CMS data over the full period 1 January 2012–30 September 2025 at all the CMS standard depths between 10 and 1945 m, in order to quantify long-term trends in temperature and salinity in the three selected regions of the Mediterranean Sea (Figures 9–11). The spatially and 10-day averaged values and the resulting linear trends at depths near 11, 399 and 1005 m are shown in Figures 12–14. The corresponding trend values, including confidence intervals, are listed in Table 2. The 399 m depth was chosen because it represents approximately the sub-surface level at which the largest differences between the Argo and CMS results are observed in the IONIAN and LEVANTINE regions. Differences in the offsets of the linear models fitted to the Argo and CMS datasets are not discussed in this paper, as the analysis focuses exclusively on the trend slopes. For the WMED, both Argo and CMS datasets show a smooth decrease in the Θ trend, from values of 0.5-0.9 °C per decade above 200 m to approximately 0.03 °C per decade near 2000 m depth (Figure 9a). Regarding salinity, results from Argo and CMS indicate a negative trend reaching –0.17 g kg^{-1} per decade near the surface, which increases with depth and changes sign, reaching a maximum of 0.11 g kg^{-1} per decade around 300 m depth (Figure 9b). Below this depth, the trend gradually decreases, reaching 0.01 g kg^{-1} per decade at 2000 m. Overall, the Argo and CMS trends are consistent, agreeing within 0.1 °C per decade for Θ and 0.01 g kg^{-1} per decade for S_A.

The regression lines are overlaid over the Argo and CMS spatially and 10-day averaged values in Figure 12. The fits are similar for Argo and CMS and the 95% confidence intervals of the trend estimates (Table 2) are generally small, except for the near-surface temperature and salinity derived from Argo floats, for which the uncertainty reaches 0.2 units per decade. This larger uncertainty is mainly due to the enhanced seasonal thermal variability in the upper water column (see Figure 12a). The coefficient of determination, R^2, is low (0.1-0.3) for both temperature and salinity at 11 m depth, mainly due to the seasonal signal. In contrast, it is consistently near 0.9 at the deeper levels. In general the goodness of fit is higher for CMS compared to Argo (higher R^2).

In the IONIAN region, the discrepancy between the Argo and CMS estimates is larger than in the WMED, particularly for temperature above 900 m, where it can reach 0.2 °C per decade (Figure 10a). Trends in Θ vary from 0.4 °C per decade (for Argo) and 0.6 °C per decade (for CMS) near the surface to 0.04 °C per

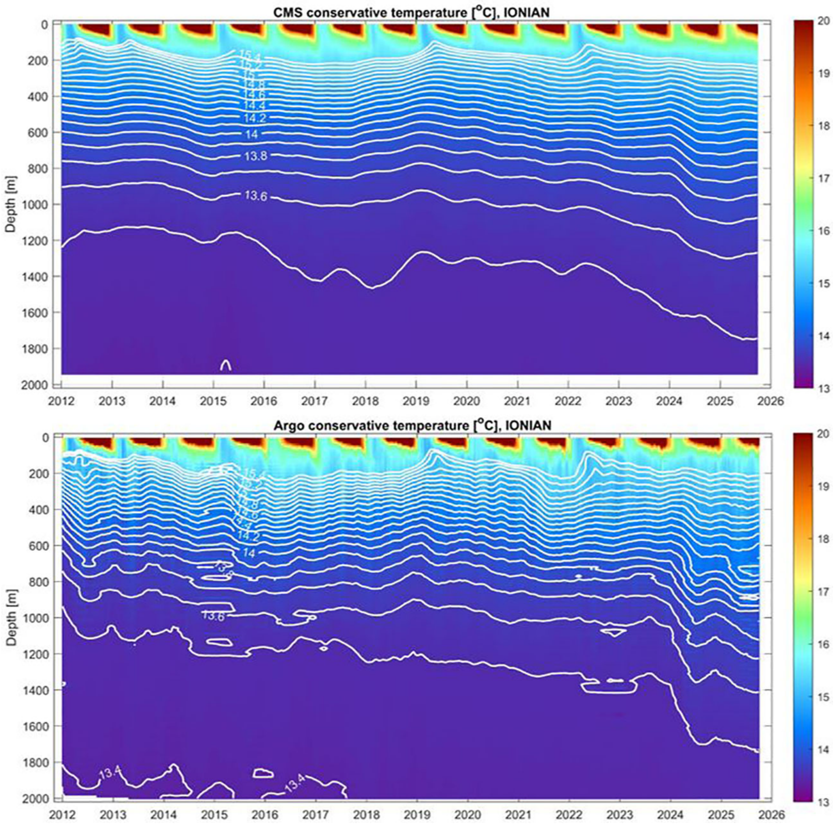

FIGURE 5
Hovmöller diagram of conservative temperature versus time and depth in the open-sea central Mediterranean area (IONIAN), derived from the CMS reanalysis (top) and Argo data (bottom). Contour interval is 0.1°C between 13.4 and 15.4°C.

decade at 2000 m depth. As in the WMED, the S_A trend is negative above 100 m, reaching –0.21 and -0.13 g kg^{-1} per decade for Argo and CMS, respectively (Figure 10b). The trend is maximal near 300 m depth (≈0.1 g kg^{-1} per decade) and gradually decreases to 0.02 g kg^{-1} per decade at 2000 m.

The scatter diagrams for both Argo and CMS in the IONIAN region (Figure 13) indicate enhanced variability in temperature and salinity throughout the water column, partially due to the spatial heterogeneity of the Argo observations, with particularly elevated values observed in 2024–2025. Despite this variability and the reduced Argo coverage, Argo and CMS regression results remain consistent below 1000 m (Figure 10). Enhanced temperature and salinity variability corresponds to a reduction of R^2 to values as low as 0.05-0.15 near the surface, and as large as 0.84 at the other deeper levels. Compared to WMED, the confidence intervals at depth are larger, but they remain approximately an order of magnitude smaller than the corresponding trend estimates (Table 2).

The LEVANTINE region has the lowest number of "independent" Argo profiles (Table 1) and exhibits significant variability, as illustrated by the substantial scatter of the temperature and salinity shown in Figure 14. As a result, 10-day averaged values and trend estimates derived from Argo and CMS data differ, particularly above 800 m depth for both Θ and S_A (Figure 11). Argo temperature trends are negative above 300 m, in contrast with the CMS estimates. Between 300 and 800 m, Argo trends can exceed the CMS values by as much as 0.2 °C per decade. For salinity, all trends are positive; however, Argo estimates can be larger than the CMS results by about 0.05 g kg^{-1} per decade near the surface. Below 800 m depth, Argo and CMS trends become consistent, showing a gradual decrease from approximately 0.07 °C per decade for Θ and 0.02 g kg^{-1} per decade for S_A to values close to zero near 2000 m depth. R^2 is generally low with a maximum between 0.3 and 0.7 at 1005 m depth. The Argo temperature trend at 11 m depth is negligible and not significant at the 95% level. In contrast, all the trend estimates are statistically significant although very different between Argo and CMS (Table 2).

4 Discussion and conclusions

This study investigated temperature and salinity changes in the Mediterranean Sea over the period 2012–2025 using Argo float profiles and CMS reanalysis products in three open-sea regions: WMED, IONIAN and LEVANTINE. The temporal evolution of Θ and S_A was assessed through Hovmöller time–depth diagrams and linear regression analysis to quantify long-term trends.

Both the Argo and CMS data reveal a consistent warming trend throughout most of the water column in the WMED region, with a maximum trend reaching 0.8-0.9 °C per decade near the surface, and a gradual decrease to 0.03 °C per decade at 2000 m (Figures 3, 9; Table 2). The propagation of heat into deeper layers may be linked

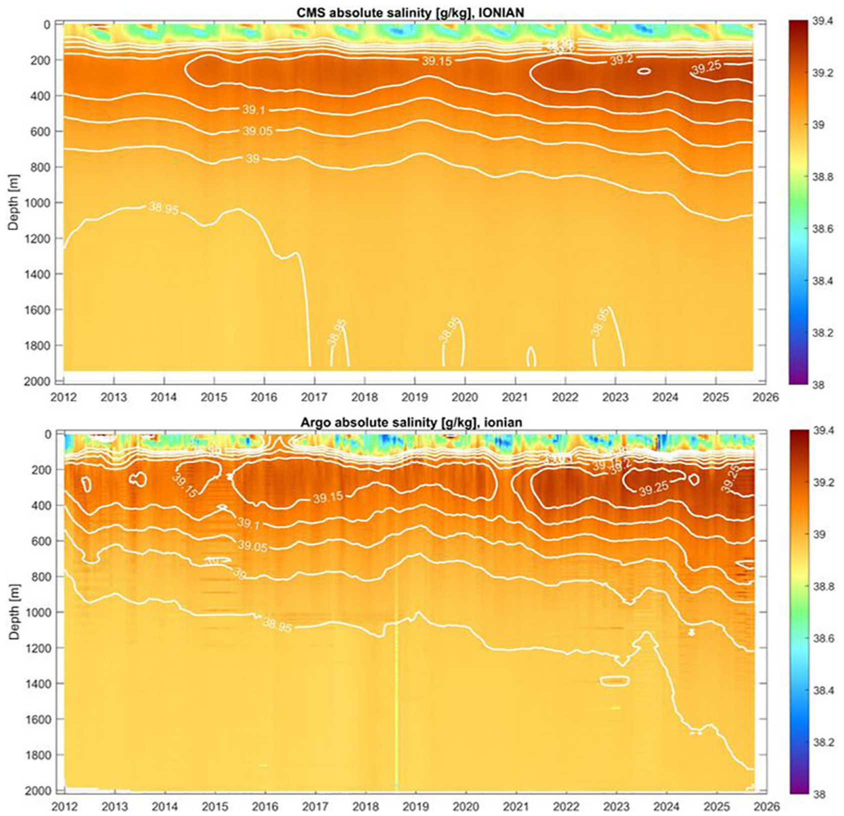

FIGURE 6
Same as Figure 5, but for absolute salinity. Contour interval is 0.05 g kg^{-1} between 38.95 and 39.25 g kg^{-1}.

to deep convection events occurring north of the study area (Margirier et al., 2020), as well as to subduction processes associated with mesoscale and sub-mesoscale circulation features (Mahadevan et al., 2020). However, the mechanisms governing vertical heat transport in the ocean are highly complex and involve a range of interacting physical processes at different scales. A detailed investigation of these dynamics lies beyond the scope of the present study.

In the IONIAN region, the vertical structure of the temperature trends is similar to that observed in the WMED, although differences between Argo and CMS estimates are apparent above 900 m depth (Figure 10). For the LEVANTINE, the discrepancy between Argo and CMS results is even larger, especially above 800 m (Figure 11). Hence, the negative Argo temperature trend observed above 300 m depth is likely an artefact of the Argo sampling and is therefore not significant. Below these depths, Argo and CMS data show consistent warming that decreases with depth. The zonal decrease in temperature trends from west to east across the water column (e.g. from 0.9 to 0.6 °C per decade for CMS near 11 m depth, see Table 2), previously reported by Chevillard et al. (2024), is confirmed by the CMS products, and partially by the Argo observations. This contrasts with estimates derived from satellite SST observations, which show maximum warming in the LEVANTINE region (e.g., García-Monteiro et al., 2022). The discrepancy between temperature trends observed at depth and those inferred from satellite measurements is expected. SST data primarily represent conditions within the thin, warm layer at the sea surface. In contrast, this near-surface layer is only partially captured by Argo floats, which generally begin sampling several meters below the surface. Consequently, reliance on SST measurements alone may provide an incomplete characterization of the Mediterranean Sea's thermal structure, potentially biasing assessments of regional warming patterns. Therefore, although both surface and subsurface temperature records offer valuable information, their combined analysis is essential for obtaining a more comprehensive understanding of the sea's thermal evolution.

Regarding salinity, a negative trend is evident in the AW (in the upper 100 m) in the WMED and IONIAN regions. This behavior is consistent with previous observations reported by Fedele et al. (2022) and is related to the freshening observed in the North Atlantic, as documented by Holliday et al. (2020). The negative trend can be as large as approximately −0.2 g kg^{-1} per decade (Figures 9, 10; Table 2). In contrast, the intermediate layers associated with the LIW show a clear increase in salinity, indicating ongoing modification of this key Mediterranean water mass (see Figures 4, 6, 9, 10). The increase rate can be as large as 0.1 g kg^{-1} per decade. In the LEVANTINE region, the LIW is near 200 m depth with a positive trend less than 0.1 g kg^{-1} per decade. At the surface, the S_A trend is about 0.15 g kg^{-1} per decade (Argo) or 0.2 g kg^{-1} per decade (CMS), as shown in Figures 8 and 11.

Most of the temperature and salinity trends estimated in this study are statistically significant. However, the main point is that Argo-derived estimates can be strongly affected by inadequate spatial and temporal sampling. More specifically, the discrepancies

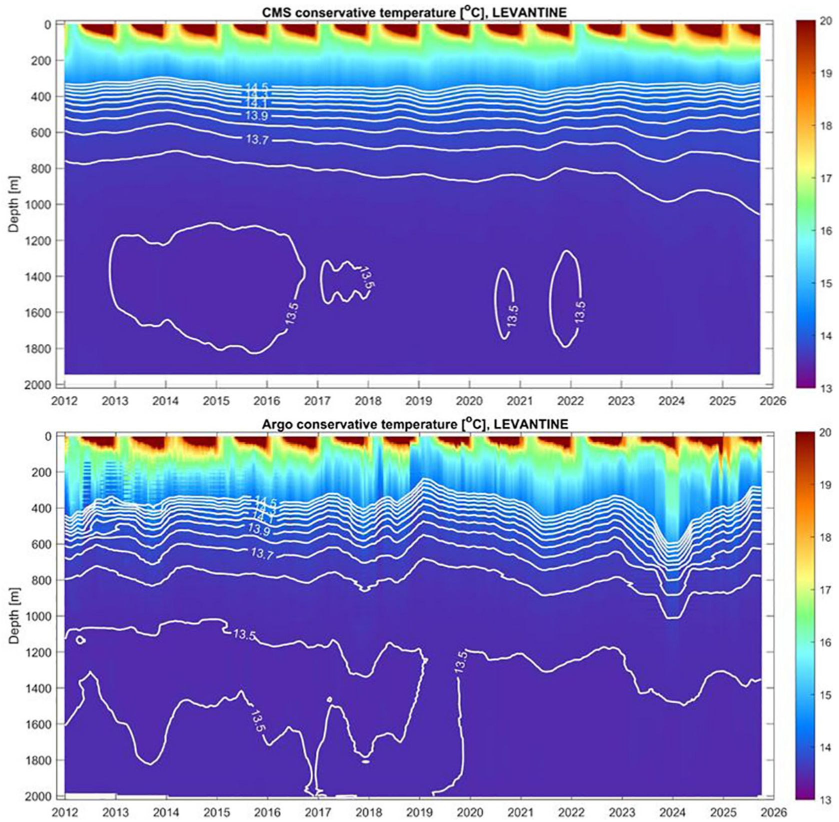

FIGURE 7
Hovmöller diagram of conservative temperature versus time and depth in the open-sea eastern Mediterranean area (LEVANTINE), derived from the CMS reanalysis (top) and Argo data (bottom). Contour interval is 0.1°C between 13.5 and 14.5°C.

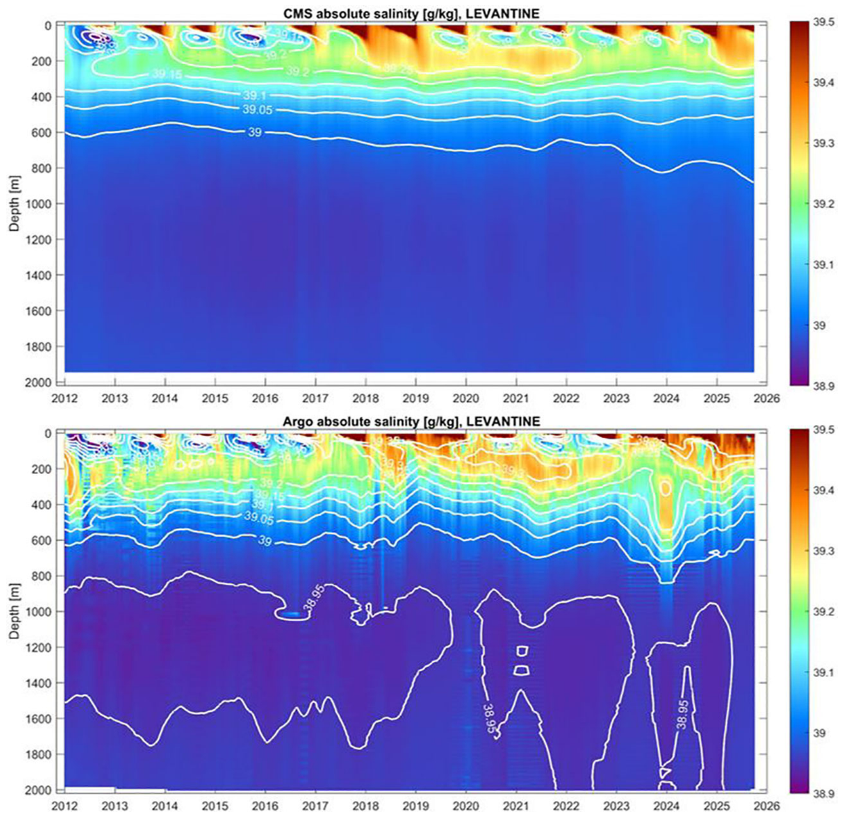

FIGURE 8
Same as Figure 7, but for absolute salinity. Contour interval is 0.05 g kg^{-1} between 38.95 and 39.35 g kg^{-1}.

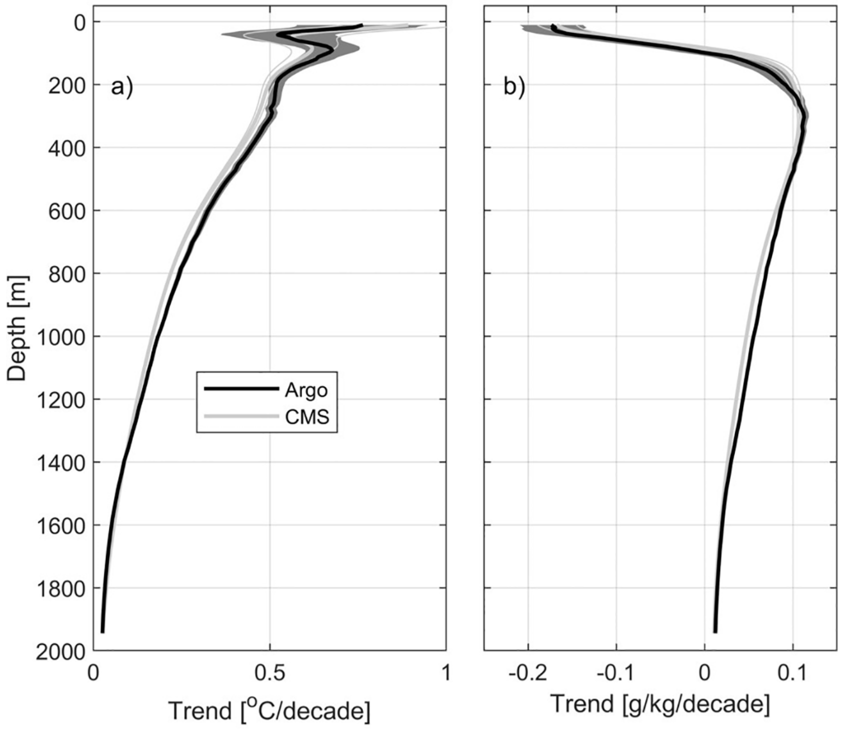

FIGURE 9
Linear trends in Θ **(a)** and S_A **(b)** as a function of depth in the WMED region, estimated from Argo (black) and CMS (grey) data. Dark grey shading indicates the 95% confidence intervals for the Argo estimates. CMS results are shown as thick light-grey lines, with corresponding confidence intervals represented by thin light-grey lines.

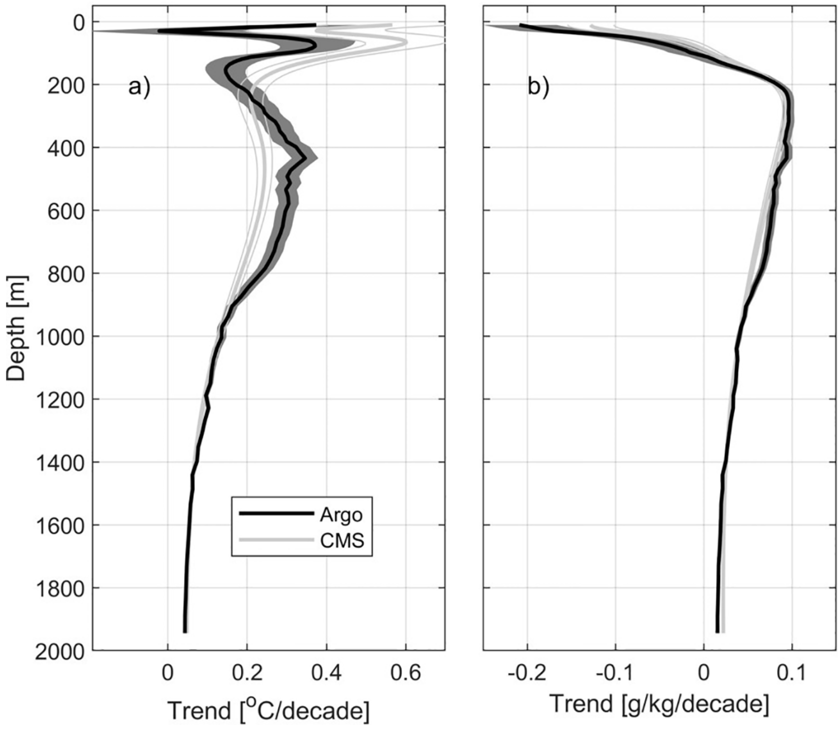

FIGURE 10
Same as in Figure 9 but for the IONIAN region.

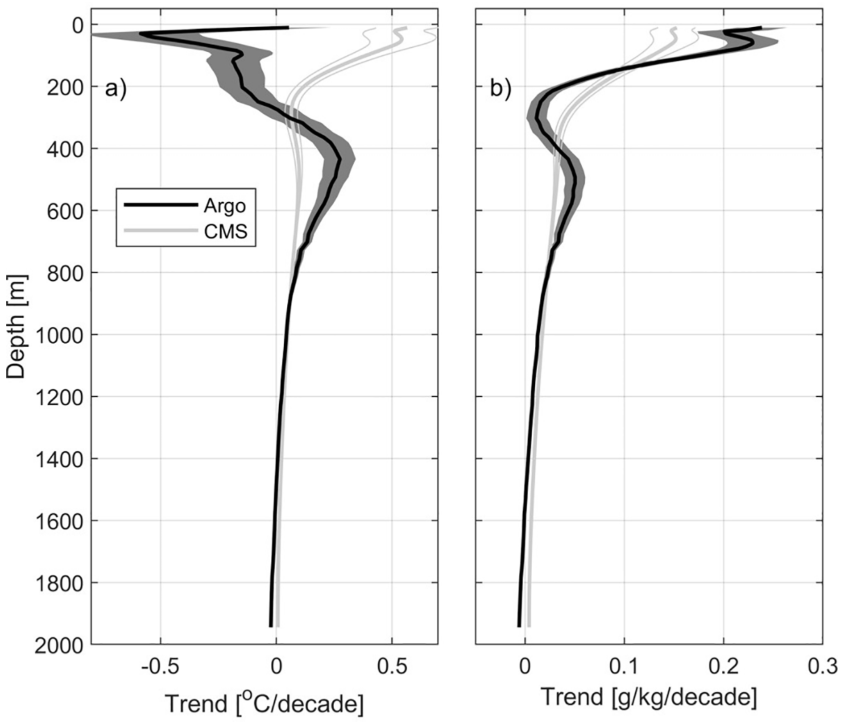

FIGURE 11
Same as in Figure 9 but for the LEVANTINE region.

between Argo and CMS trends in the IONIAN and LEVANTINE regions are significant in the upper layers of the water column. CMS temperature trends significantly exceed those found with Argo data in these regions. In contrast, Argo salinity trends are larger compared to reanalysis in the upper LEVANTINE region, but they are comparable in the surface IONIAN region. Although collocated and simultaneous Argo and CMS profiles can differ—particularly near the surface (see Appendix 1)—we believe that the trend discrepancies are primarily due to the sampling limitations of the Argo network. Sparse and non-uniform float distribution introduces sampling bias, especially in regions dominated by strong and persistent mesoscale variability. Under such conditions, a limited number of profiles may not be representative of the regional mean state, leading to significant uncertainties in trend estimates. These results have important implications for the design and optimization of the Mediterranean observing system.

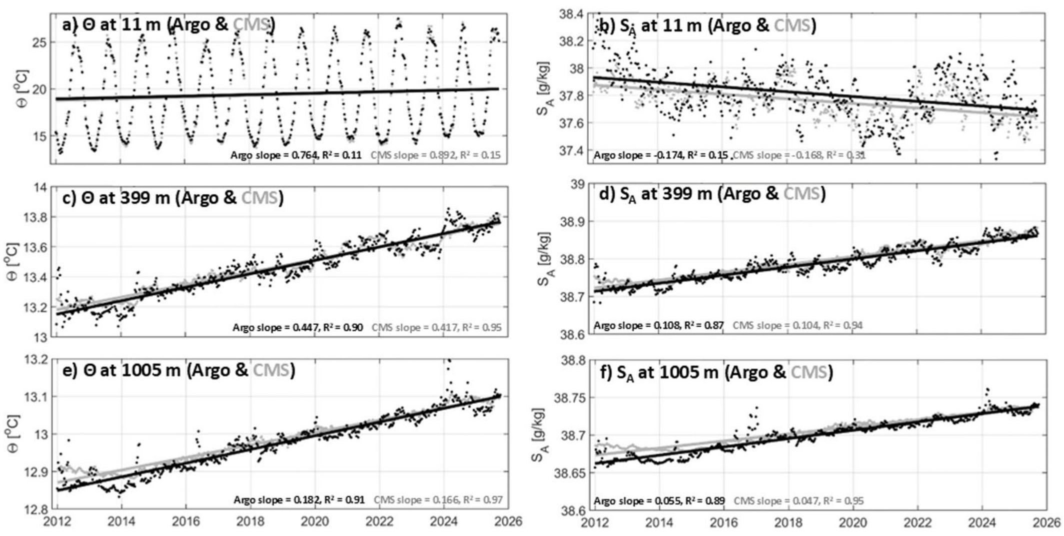

FIGURE 12
Conservative temperature [Θ; **(a, c, e)**] and absolute salinity [S_A; **(b, d, f)**] at depths of 11, 399, and 1005 m, averaged over 10-day intervals in the WMED region. Argo and CMS estimates are shown in black and grey, respectively. The corresponding linear trends are also displayed, together with the associated slopes and coefficients of determination (R^2).

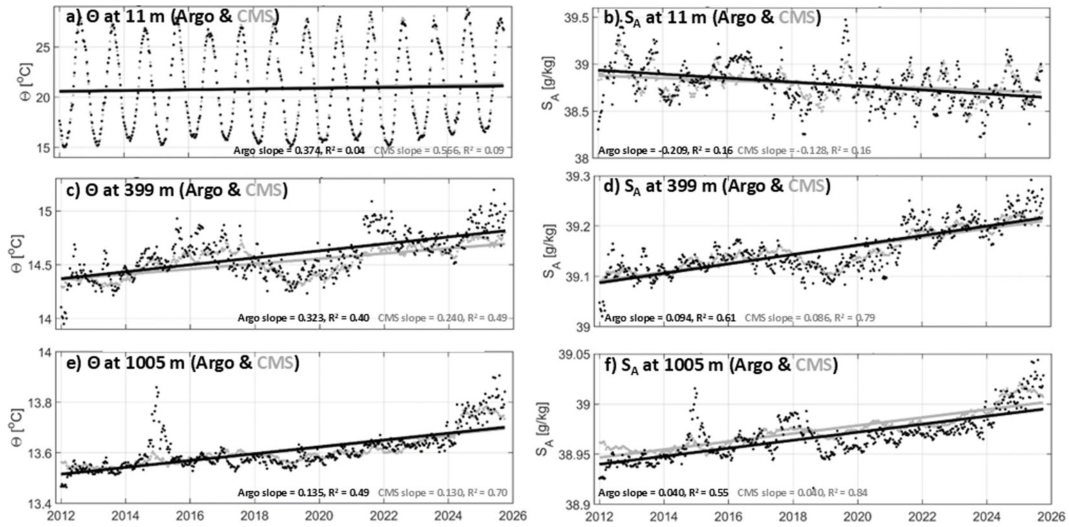

FIGURE 13
Same as in Figure 12 but for the IONIAN region.

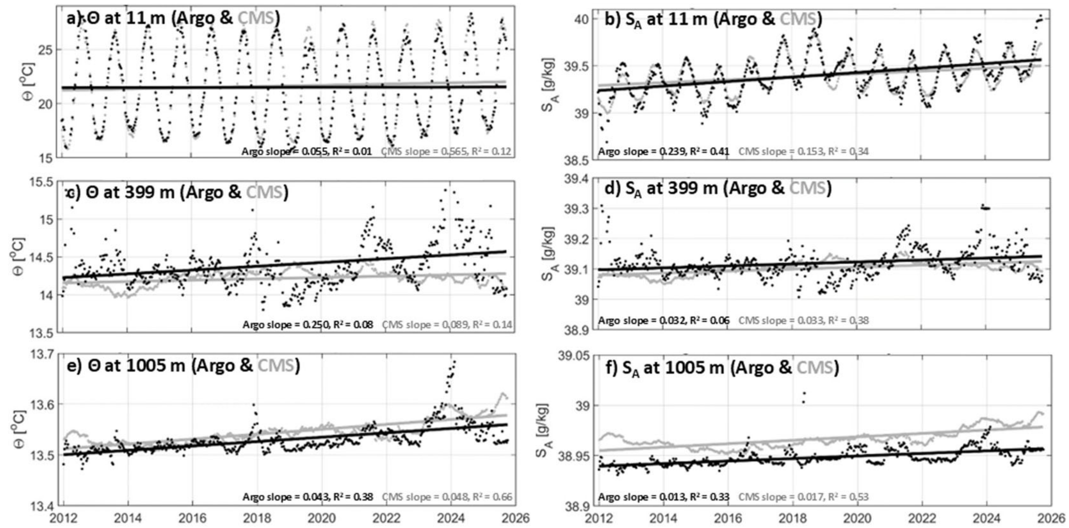

FIGURE 14
Same as in Figure 12 but for the LEVANTINE region.

TABLE 2 **Long-term trends (slope of linear fit, with 95% confidence intervals) for conservative temperature Θ and absolute salinity S_A at 11, 399 and 1005 m depth, in the WMED, IONIAN and LEVANTINE regions, as derived from Argo and CMS data. Insignificant trends are listed in italic.**

Region	Depth [m]	Argo		CMS	
		Θ slope [°C decade^{-1}]	S_A slope [g kg^{-1} decade^{-1}]	Θ slope [°C decade^{-1}]	S_A slope [g kg^{-1} decade^{-1}]
WMED	11	0.764 ± 0.188	-0.174 ± 0.036	0.892 ± 0.185	-0.168 ± 0.022
	399	0.447 ± 0.013	0.108 ± 0.004	0.417 ± 0.008	0.104 ± 0.002
	1005	0.182 ± 0.005	0.055 ± 0.002	0.166 ± 0.003	0.047 ± 0.001
IONIAN	11	0.374 ± 0.168	-0.209 ± 0.042	0.566 ± 0.162	-0.128 ± 0.026
	399	0.323 ± 0.035	0.094 ± 0.007	0.240 ± 0.022	0.086 ± 0.004
	1005	0.135 ± 0.012	0.040 ± 0.003	0.130 ± 0.008	0.040 ± 0.002
LEVANTINE	11	*0.055 ± 0.184*	0.239 ± 0.025	0.565 ± 0.135	0.153 ± 0.019
	399	0.250 ± 0.076	0.032 ± 0.011	0.089 ± 0.019	0.033 ± 0.004
	1005	0.043 ± 0.005	0.013 ± 0.002	0.048 ± 0.003	0.017 ± 0.001

We aimed to exclude Argo data within significant mesoscale eddies, as identified in satellite altimetry maps, to minimize their influence on long-term trend estimates. However, the high prevalence of these structures led to a substantial reduction in the number of usable Argo profiles, resulting in inconclusive trend results. To ensure the robustness of our findings, we compared various least squares fitting methods (see Appendix 2) and evaluated the sensitivity of our results to the size of the open-sea domains considered (see Appendix 3). These analyses revealed that the trends derived from Argo data in the Western Mediterranean are robust and comparable to those obtained from the CMS data. In contrast, in the Central and Eastern Mediterranean, discrepancies between the Argo and CMS results may be significant, especially in the upper water column, largely due to the sparse Argo sampling in those areas.

It is important to highlight that the Argo dataset and the CMS reanalysis products are not independent, and the latter cannot be considered a true reference dataset. In cases where the model outputs and Argo results converge, such as in the Western Mediterranean, the consistency between the two enhances confidence in the findings. Conversely, instances where the results diverge call for further investigation into the potential causes of these discrepancies, as well as an examination of the limitations and uncertainties associated with both datasets.

The results reported in this paper indicate that the capability of the Argo network to detect long-term thermohaline trends strongly depends not only on the total number of profiles, but also on their spatial and temporal distribution. In dynamically active regions such as the Levantine and Ionian subbasins, higher float density and more uniform sampling are required to adequately resolve variability and obtain robust trend estimates. Conversely, in well-sampled regions such as the Western Mediterranean, the current Argo configuration appears sufficient to monitor long-term changes. These findings highlight the need for targeted deployment strategies aimed at reducing sampling gaps and improving coverage in undersampled areas.

Overall, the analysis confirms that the Mediterranean Sea continues to experience significant warming and subsurface salinification, extending the findings of previous studies such as Fedele et al. (2022); Kubin et al. (2023), and Chevillard et al. (2024). The warming trends reaching 0.8-0.9 °C per decade near the surface in the western Mediterranean are significantly larger than those reported in the literature. The contrasting negative salinity trend associated with the near-surface AW (–0.2 g kg^{-1} per decade) and the positive trend related to the subsurface LIW (0.1 g kg^{-1} per decade) represent an important and novel result highlighted by this study. The persistence of these trends through 2025 highlights the continued impact of ongoing global climate change on the Mediterranean thermohaline structure. It is therefore strongly recommended to continue the Argo monitoring in the Mediterranean Sea, with special effort to sample all areas as uniformly as possible.

Data availability statement

The datasets for this study were downloaded from the Argo and CMS web sites. CMS data were downloaded in December 2025 from https://data.marine.copernicus.eu/product/MEDSEA_MULTIYEAR_PHY_006_004. Argo float data and metadata were downloaded from the Argo Global Data Assembly Centre (GDAC) in January 2026 (https://doi.org/10.17882/42182, https://erddap.ifremer.fr/erddap/tabledap/ArgoFloats.html).

Author contributions

P-MP: Investigation, Writing – review & editing, Writing – original draft, Conceptualization, Visualization, Formal analysis, Data curation, Methodology. GN: Funding acquisition, Data curation, Project administration, Writing – review & editing, Conceptualization. AG: Data curation, Writing – review & editing. EM: Funding acquisition, Writing – review & editing, Project administration.

Funding

The author(s) declared that financial support was received for this work and/or its publication. This research was mainly financed by the Italian Ministry of University and Research, as part of the Argo-Italy program.

Acknowledgments

The authors are grateful to Antonio Bussani for helping with the CMS data handling, and to the reviewers for providing constructive comments on the original manuscript. The Mediterranean Argo data used in this study were collected and made freely available by the International Argo Program and the national programs that contribute to it. (https://argo.ucsd.edu, https://www.ocean-ops.org). The Argo Program is part of the Global Ocean Observing System.

Conflict of interest

The author(s) declared that this work was conducted in the absence of any commercial or financial relationships that could be construed as a potential conflict of interest.

The reviewer MB declared a past co-authorship with the author P-MP to the handling editor.

Generative AI statement

The author(s) declared that generative AI was not used in the creation of this manuscript.

Any alternative text (alt text) provided alongside figures in this article has been generated by Frontiers with the support of artificial intelligence and reasonable efforts have been made to ensure accuracy, including review by the authors wherever possible. If you identify any issues, please contact us.

Publisher's note

All claims expressed in this article are solely those of the authors and do not necessarily represent those of their affiliated organizations, or those of the publisher, the editors and the reviewers. Any product that may be evaluated in this article, or claim that may be made by its manufacturer, is not guaranteed or endorsed by the publisher.

Supplementary material

The Supplementary Material for this article can be found online at: https://www.frontiersin.org/articles/10.3389/fmars.2026.1846069/full#supplementary-material

SUPPLEMENTARY FIGURE 1
Mean difference (or bias, Argo minus CMS) versus depth between conservative temperature Θ **(a)** and absolute salinity S_A **(b)** from Argo floats and CMS sampled at the float times and locations, over the three regions considered for the entire year 2015.

SUPPLEMENTARY FIGURE 2
Same as in Supplementary Figure 1 but for the RMSD.

SUPPLEMENTARY FIGURE 3
Linear trends in Θ **(a)** and S_A **(b)** as a function of depth in the WMED region, estimated from Argo observations using different methods: (i) ordinary least-squares fitting applied to spatially averaged values over 10-day intervals (black); (ii) weighted least-squares fitting, with weights proportional to the number of observations within each 10-day interval in the WMED region (red); and (iii) ordinary least-squares fitting applied to all individual profiles in the region, excluding profiles with identical times (blue; barely visible because the results are very similar to those obtained with method ii).

SUPPLEMENTARY FIGURE 4
Same as in Supplementary Figure 3 but for the IONIAN region.

SUPPLEMENTARY FIGURE 5
Same as in Supplementary Figure 3 but for the LEVANTINE region.

SUPPLEMENTARY FIGURE 6
Linear trends in Θ **(a)** and S_A **(b)** versus depth, as estimated with Argo profiles (green dots) in the reduced (red), regular (black), and extended (blue) WMED regions shown in the insert. The number of Argo profiles in the regions is listed.

SUPPLEMENTARY FIGURE 7
Same as in Supplementary Figure 6 but for the reduced, regular, and extended IONIAN regions shown in the insert.

SUPPLEMENTARY FIGURE 8
Same as in Supplementary Figure 6 but for the reduced, regular, and extended LEVANTINE regions shown in the insert.

References

Argo float data and metadata from Global Data Assembly Centre (Argo GDAC) (2026). Argo float data and metadata from Global Data Assembly Centre (Argo GDAC). doi: 10.17882/42182

Aydogdu, A., Miraglio, P., Escudier, R., Clementi, E., and Masina, S. (2023). The dynamical role of upper layer salinity in the Mediterranean Sea. *State Planet.* 1, 1–9. doi: 10.5194/sp-2022-11

Béthoux, J. P., Gentili, B., Raunet, J., and Tailliez, D. (1990). Warming trend in the western Mediterranean deep water. *Nature* 347, 660–662. doi: 10.1038/347660a0

Borghini, M., Bryden, H., Schroeder, K., Sparnocchia, S., and Vetrano, A. (2014). The Mediterranean is becoming saltier. *Ocean Sci.* 10, 693–700. doi: 10.5194/os-10-693-2014

Chevillard, C., Juza, M., Dıaz-Barroso, L., Reyes, E., Escudier, R., and Tintoré, J. (2024). Capability of the Mediterranean Argo network to monitor sub-regional climate change indicators. *Front. Mar. Sci.* 11, 1416486. doi: 10.3389/fmars.2024.1416486

Emery, W. J., and Thomson, R. E. (2024). "Data analysis methods in physical oceanography," in *Elsevier Science, Amsterdam*. doi: 10.1016/C2021-0-00298-4

Escudier, R., Clementi, E., Cipollone, A., Pistoia, J., Drudi, M., Grandi, A., et al. (2021). A high resolution reanalysis for the Mediterranean Sea. *Front. Earth Sci.* 9, 1060. doi: 10.3389/feart.2021.702285

Escudier, R., Clementi, E., Nigam, T., Aydogdu, A., Fini, E., Pistoia, J., et al. (2025). Mediterranean Sea Production Centre MEDSEA_MULTIYEAR_PHY_006_004. Quality information document. MEMS-MED-QUID-006-004, 28 May 2025, 2.4, pp 67.

Escudier, R., Clementi, E., Omar, M., Cipollone, A., Pistoia, J., Aydogdu, A., et al. (2020). "Mediterranean sea physical reanalysis (CMEMS MED-currents) (Version 1) [Data set," in *Copernicus Monitoring Environment Marine Service (Cmems)*. doi: 10.25423/CMCC/MEDSEA_MULTIYEAR_PHY_006_004_E3R1

Fedele, G., Mauri, E., Notarstefano, G., and Poulain, P. M. (2022). Characterization of the Atlantic Water and Levantine Intermediate Water in the Mediterranean Sea using 20 years of Argo data. *Ocean Sci.* 18, 129–142. doi: 10.5194/os-18-129-2022

García-Monteiro, S., Sobrino, J. A., Julien, Y., Sòria, G., and Skokovic, D. (2022). Surface temperature trends in the Mediterranean Sea from MODIS data during years 2003–2019. *Reg. Stud. Mar. Sci.* 49, 102086. doi: 10.1016/j.rsma.2021.102086

Giorgi, F. (2006). Climate change hot-spots. *Geophys. Res. Lett.* 33. doi: 10.1029/2006GL025734

Holliday, N. P., Bersch, M., Berx, B., Chafik, L., Cunningham, S., Florindo-López, C., et al. (2020). Ocean circulation causes the largest freshening event for 120 years in eastern subpolar North Atlantic. *Nat. Commun.* 11, 585. doi: 10.1038/s41467-020-14474-y

Juza, M., and Tintoré, J. (2021). Multivariate sub-regional ocean indicators in the Mediterranean Sea: From event detection to climate change estimations. *Front. Mar. Sci.* 8, 610589. doi: 10.3389/fmars.2021.610589

Kassis, D., and Korres, G. (2020). Hydrography of the Eastern Mediterranean basin derived from argo floats profile data. *Deep Sea Res. II* 171, 104712. doi: 10.1016/j.dsr2.2019.104712

Krahmann, G., and Schott, F. (1998). Longterm increases in Western Mediterranean salinities and temperatures: Anthropogenic and climatic sources. *Geophys. Res. Lett.* 25, 4209–4212. doi: 10.1029/1998GL900143

Kubin, E., Menna, M., Mauri, E., Notarstefano, G., Mieruch, S., and Poulain, P. M. (2023). Heat content and temperature trends in the Mediterranean Sea as derived from Argo float data. *Front. Mar. Sci.* 10. doi: 10.3389/fmars.2023.1271638

Mahadevan, A., Pascual, A., Rudnick, D. L., Ruiz, S., Tintoré, J., and D'Asaro, E. (2020). Coherent pathways for vertical transport from the surface ocean to interior. *Bull. Am. Meteorol. Soc* 101, E1996–E2004. doi: 10.1175/bams-d-19-0305.1

Margirier, F., Testor, P., Heslop, E., Mallil, K., Bosse, A., Houpert, L., et al. (2020). Abrupt warming and salinification of intermediate waters interplays with decline of deep convection in the Northwestern Mediterranean Sea. *Sci. Rep.* 10, 20923. doi: 10.1038/s41598-020-77859-5

Merchant, C. J., Allan, R. P., and Embury, O. (2025). Quantifying the acceleration of multidecadal global sea surface warming driven by Earth's energy imbalance. *Env. Res. Lett.* 20, 024037. doi: 10.1088/1748-9326/adaa8a

Millot, C. (2007). Interannual salinification of the Mediterranean inflow. *Geophys. Res. Lett.* 34, L21609. doi: 10.1029/2007GL03117

Mohamed, B., Abdallah, A. M., Alam El-Din, K., Nagy, H., and Shaltout, M. (2019). Inter-annual variability and trends of sea level and sea surface temperature in the Mediterranean Sea over the last 25 years. *Pure Appl. Geophys.* 176, 3787–3810. doi: 10.1007/s00024-019-02156-w

Napolitano, E., Carillo, A., Iacono, R., Struglia, M. V., dell'Aquila, A., Palma, M., et al. (2025). Unprecedented Mediterranean Sea warming in 2024: Analysis of the driving mechanisms. *Front. Mar. Sci.* 12, 1668204. doi: 10.3389/fmars.2025.1668204

Nykjaer, L. (2009). Mediterranean Sea surface warming 1985–2006. *Clim. Res.* 39, 11–17. doi: 10.3354/cr00794

Oddo, P., Adani, M., Carere, F., Cipollone, A., Goglio, A. C., Jansen, E., et al. (2026). Implementation and evaluation of sea level operators in OceanVar2.0: An open-source oceanographic three-dimensional variational data assimilation system. *Geosci. Model. Dev.* 19, 423–445. doi: 10.5194/gmd-19-423-2026

Pastor, F., Valiente, J. A., and Khodayar, S. (2020). A warming Mediterranean: 38 years of increasing sea surface temperature. *Remote Sens.* 12, 2687. doi: 10.3390/rs12172687

Pisano, A., Marullo, S., Artale, V., Falcini, F., Yang, C., Leonelli, F. E., et al. (2020). New evidence of Mediterranean climate change and variability from sea surface temperature observations. *Remote Sens.* 12, 132. doi: 10.3390/rs12010132

Poulain, P. M., Barbanti, R., Font, J., Cruzado, A., Millot, C., Gertman, I., et al. (2007). MedArgo: A drifting profiler program in the Mediterranean Sea. *Ocean Sci.* 3, 379–395. doi: 10.5194/os-3-379-2007

Robinson, A. R., Golnaraghi, M., Leslie, W. G., Artegiani, A., Hecht, A., Lazzoni, E., et al. (1991). The eastern Mediterranean general circulation: Features, structure and variability. *Dyn. Atmos. Oceans* 15, 215–240. doi: 10.1016/0377-0265(91)90021-7

Skliris, N., Sofianos, S., Gkanasos, A., Mantziafou, A., Vervatis, V., Axaopoulos, P., et al. (2012). Decadal scale variability of sea surface temperature in the Mediterranean Sea in relation to atmospheric variability. *Ocean Dyn.* 62, 13–30. doi: 10.1007/s10236-011-0493-5

Skliris, N., Zika, J. D., Herold, L., Josey, S. A., and Marsh, R. (2018). Mediterranean sea water budget long-term trend inferred from salinity observations. *Clim. Dyn.* 51, 2857–2876. doi: 10.1088/1748-9326/aace42

Vargas-Yáñez, M., García-Martínez, M. C., Moya, F., Balbín, R., López-Jurado, J. L., Serra, M., et al. (2017). Updating temperature and salinity mean values and trends in the Western Mediterranean: The RADMED project. *Prog. Oceanogr.* 127, 27–46. doi: 10.1016/j.pocean.2017.09.004

Wong, A. P. S., Wijffels, S. E., Riser, S. C., Pouliquen, S., Hosoda, S., Roemmich, D., et al. (2020). Argo data 1999–2019: Two million temperature-salinity profiles and subsurface velocity observations from a global array of profiling floats. *Front. Mar. Sci.* 7, 700. doi: 10.3389/fmars.2020.00700

Appendix

Appendix 1: comparing Argo and CMS data at the float times and locations

The temperature and salinity profiles of Argo and CMS sampled at the specific times and locations of the floats are compared for the selected year, 2015, abundant in Argo float data, over the three Mediterranean regions. Differences are assessed in terms of bias, mean difference Argo minus CMS (Supplementary Figure 1), and root mean squared difference (RMSD; Supplementary Figure 2).

Below 200 m depth, the mean difference, or bias, is bounded by 0.05 °C for temperature and 0.01 g kg^{-1} for salinity (Supplementary Figure 1). Near the surface the bias can be as high as 0.1 °C and 0.05 g kg^{-1}, mainly due to the higher variability in the upper layer.

In terms of RMSD (Supplementary Figure 2), maximum values occur near the surface with up to 1 °C and 0.24 g kg^{-1}. Below 200 m depth, they are limited to 0.3 °C and 0.1 g kg^{-1}.

The discrepancies observed between collocated and contemporaneous Argo and CMS data are similar in the three regions considered. They can be attributed to the OceanVAR assimilation methodology, which generally smooths profiles that display significant variability. Additionally, CMS data are produced daily with a spatial resolution of approximately 5 km, while Argo profiles consist of pointwise measurements taken at specific, intermittent times.

Appendix 2: comparing linear trend methods

Three least-squares fitting approaches are compared in this section using Argo data from the WMED, IONIAN, and LEVANTINE regions:

i. Ordinary least-squares fitting applied to spatially averaged values over 10-day intervals within each region.
ii. Weighted least-squares fitting applied to spatially and temporally averaged values, with weights proportional to the number of observations within each 10-day interval in each region.
iii. Ordinary least-squares fitting applied to individual observations, excluding profiles with identical times.

The results are shown in Supplementary Figures 3–5. Note that methods (ii) and (iii) yield very similar results, as they are approximately equivalent in a mathematical sense.

In the WMED region (Supplementary Figure 3), trend differences among methods are generally modest but can reach up to approximately 0.03 units for both Θ and S_A, primarily above 300 m depth. In the IONIAN region (Supplementary Figure 4), salinity trends remain broadly consistent across methods, whereas temperature trends show larger discrepancies above 800 m depth, reaching up to 0.08 °C per decade. In the LEVANTINE region (Supplementary Figure 5), differences between methods (i) and (ii) are also significant above 800 m depth, with values reaching up to 0.4 °C per decade for temperature and 0.03 g kg^{-1} per decade for salinity.

Appendix 3: sensitivity to the size of the geographical areas considered

Linear trends in Θ and S_A were also estimated for reduced and extended regions, defined by subtracting or adding 0.25° to the geographical limits listed in Table 1. As shown in Supplementary Figures 1–3, the number of Argo profiles differs substantially among the reduced, standard, and extended geographical domains.

In the WMED region (Supplementary Figure 6), trend estimates are generally comparable below 300 m depth. Above this depth, however, differences reach up to 0.05 °C per decade and 0.03 g kg^{-1} per decade. In particular, the extended region exhibits a weaker temperature trend and a stronger salinity trend compared to the standard and reduced domains.

In the IONIAN region (Supplementary Figure 7), discrepancies among trend estimates are more pronounced and extend deeper into the water column, down to approximately 1400 m depth. Differences can reach up to 0.05 °C per decade and 0.05 g kg^{-1} per decade. The reduced region again shows a weaker salinity trend, while temperature differences above 400 m and below 600 m display opposite signs.

For the LEVANTINE region (Supplementary Figure 8), significant differences are mainly confined to the upper 800 m of the water column, with maximum deviations of approximately 0.05 °C per decade for temperature and 0.01 g kg^{-1} per decade for salinity.

Overall, modifying the geographical boundaries by ±0.25° results in variations of up to 0.05 units in the estimated trends of both Θ and S_A across all regions.